Supporting Information

Continuous Stirred-Tank Reactor Cascade Platform for Self- Optimization of Reactions Involving Solids

Kakasaheb Y. Nandiwale[a], Travis Hart[a], Andrew F. Zahrt[a], Anirudh M. K. Nambiar[a], Prajwal T. Mahesh[a], Yiming Mo[a], María José Nieves-Remacha[b], Martin D. Johnson[c], Pablo García-Losada, Carlos Mateos[b], Juan A. Rincón[b] and Klavs F. Jensen[*a]

[a]Department of Chemical Engineering, Massachusetts Institute of Technology, 77 Massachusetts Avenue, Cambridge, Massachusetts 02139, United States.

[b]Centro de Investigación Lilly S.A., Avda. de la Industria 30, Alcobendas-Madrid 28108, Spain.

[c]Small Molecule Design and Development, Eli Lilly and Company, Indianapolis, Indiana 46285, United States

*Correspondence to:
kfjensen@mit.edu

Table of Contents

Photoreactor fabrication and characterization with chemical actinometry

The fabricated photo CSTR cascade with Peltier cooler and blue LED array is shown in Figure S1(a-d). The photoreactor consists of three, 1.5 W, 455 nm blue LEDs, which sit in front of each CSTR cascade well to maximize absorbed photon flux.
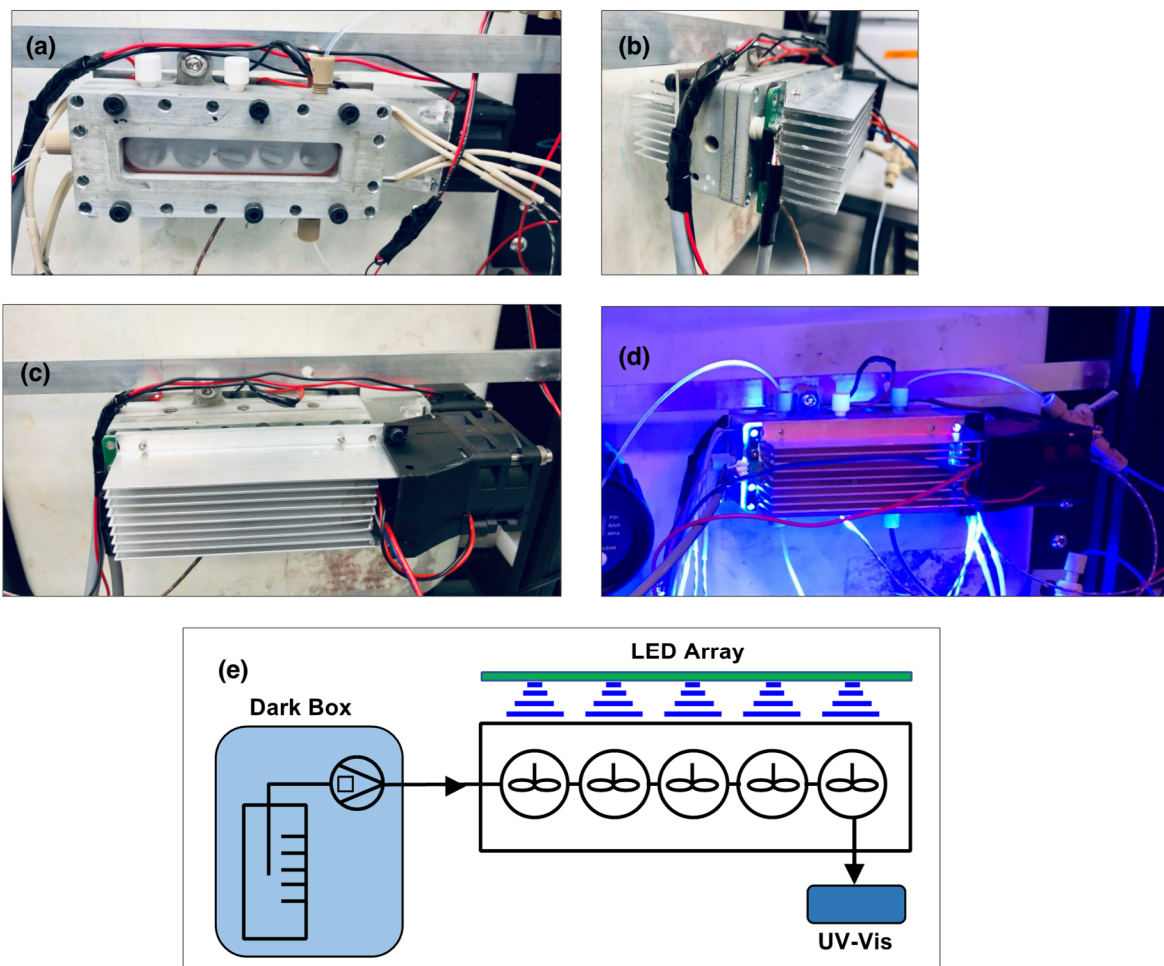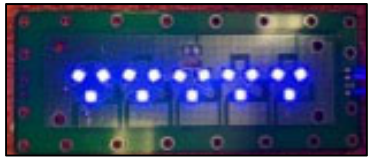
Figure S1. (a) CSTR cascade with Peltier cooler mounted at the backside, (b) Side view of photo CSTR cascade sandwiched between the Peltier cooler with heat sink and LED array with heat sink, (c) Front view of photoreactor, (d) Photoreactor with LED array, and (e) Schematic of setup used for the chemical actinometry.

Chemical actinometry was performed to measure an actual absorbed photon flux in a specific reactor volume [Figure S1 (e)]. Oxidation of 9,10-diphenylantracene (0.1 mM) with 0.2 mM

Ru(bpy)$_3$Cl$_2$ in acetonitrile was used as a chemical actinometer. Further details about the design of CSTR cascade and chemical actinometry can be found in our previous publications.[1, 2]

The absorbed photon flux obtained with conventional 40 W blue LED (Kessil lightening A160 WE) was compared with the newly developed photoreactor with LED array (Table S1).

Table S1. Absorbed photon flux obtained for CSTR cascade using different types LED.

LED Brightness (%)	Absorbed photon flux (mol s^{-1} m^{-3})	
	Blue LED (40 W)	LED Array (22.5 W)
10	0.08	0.10
25	0.09	0.11

The efficiency of Peltier cooler to control temperature of photo CSTR cascade is evaluated at the different LED brightness (Table S1).

Table S2. Photo CSTR cascade temperature with Peltier cooler at different LED brightness

Peltier Cooler Set Temp. (°C)	CSTR Cascade Temp. (°C) (100% LED brightness)	CSTR Cascade Temp. (°C) (LED OFF)
35	35	35
20	20	20
15	18	15
5	17	8
0	17	7

Experimental setup for automated reaction optimization

Experimental setup of automated optimization system with various components necessary to perform optimization of reaction containing solids is shown in Figure S2.
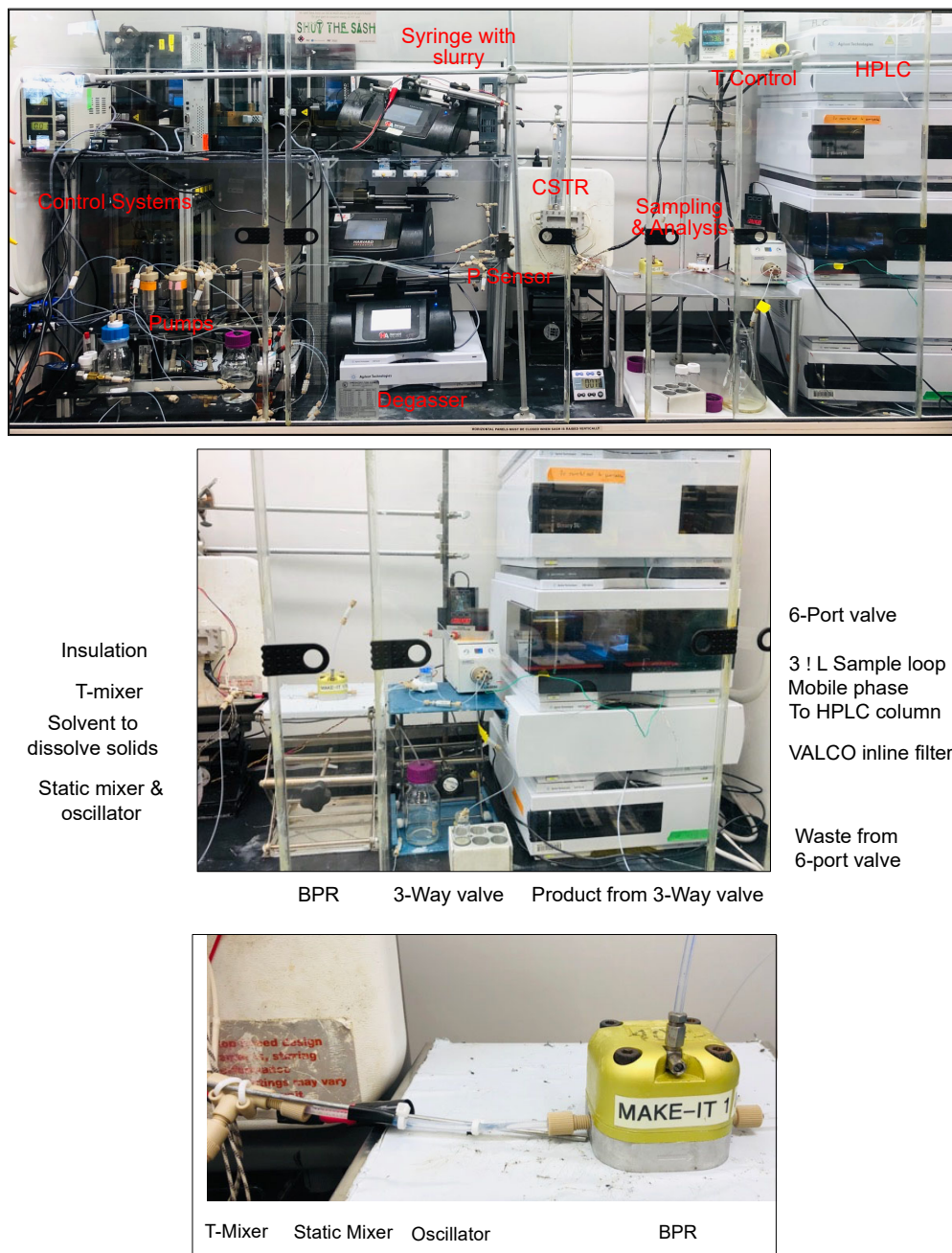

Figure S2: Photographs of the automated optimization system showing the various components necessary to run automated optimization of reaction containing solids.

Key Components with model number (Figure S2): magnetic tumbler/stirrers (V&P Scientific VP 710D3-4), oscillator (Model No. 306-10H, Precision Microdrives), syringe pumps (Harvard Apparatus PHD Ultra), positive displacement pump (VICI, Model M6/M50 pump), back-pressure regulator (Model No. BPR-10, Zaiput Flow Technologies), pressure controller (Model No. PCD-500PSIG-D, Alicat Scientific).

Automated optimization system startup and operation

The system is turned on after connecting all the required hardware to run the automated reaction optimization. The hardware communication is established by starting the virtual instrument (VI) in the LabVIEW (Figure S3 and Figure S4). Inline sampling by using set of 3-way valve and 6-port two position valve is automated with the LabVIEW control. The online HPLC is also set up to trigger the method start with the LabVIEW control by using relay. The LabVIEW VI has two main tabs, one to show all the controls, warning indicators, COM port connections, data paths, flow rates, inline sampling time, and online HPLC analysis time, automated experimentation time, and data analysis (Figure S3). The second tab shows optimization variables, algorithm settings, reagent location and types (slurry/homogeneous), and the DoE table with the experimental progress (Figure S4). The LabVIEW VI user interface also indicates warnings about the reactor temperature and reactor pressure monitored by the thermocouple, and inline pressure sensor, respectively. It also has a capability to notify the user about any errors and warnings in the system while running an optimization campaign. The LabVIEW VI is also written to save the optimization data log file while performing the automated DoE and experimentation during the course of reaction-self optimization (Figure S3). This data log file can be used to resume/restore the DoE

experiments, if paused during the automated optimization campaign for the reagent refill or any other reason.
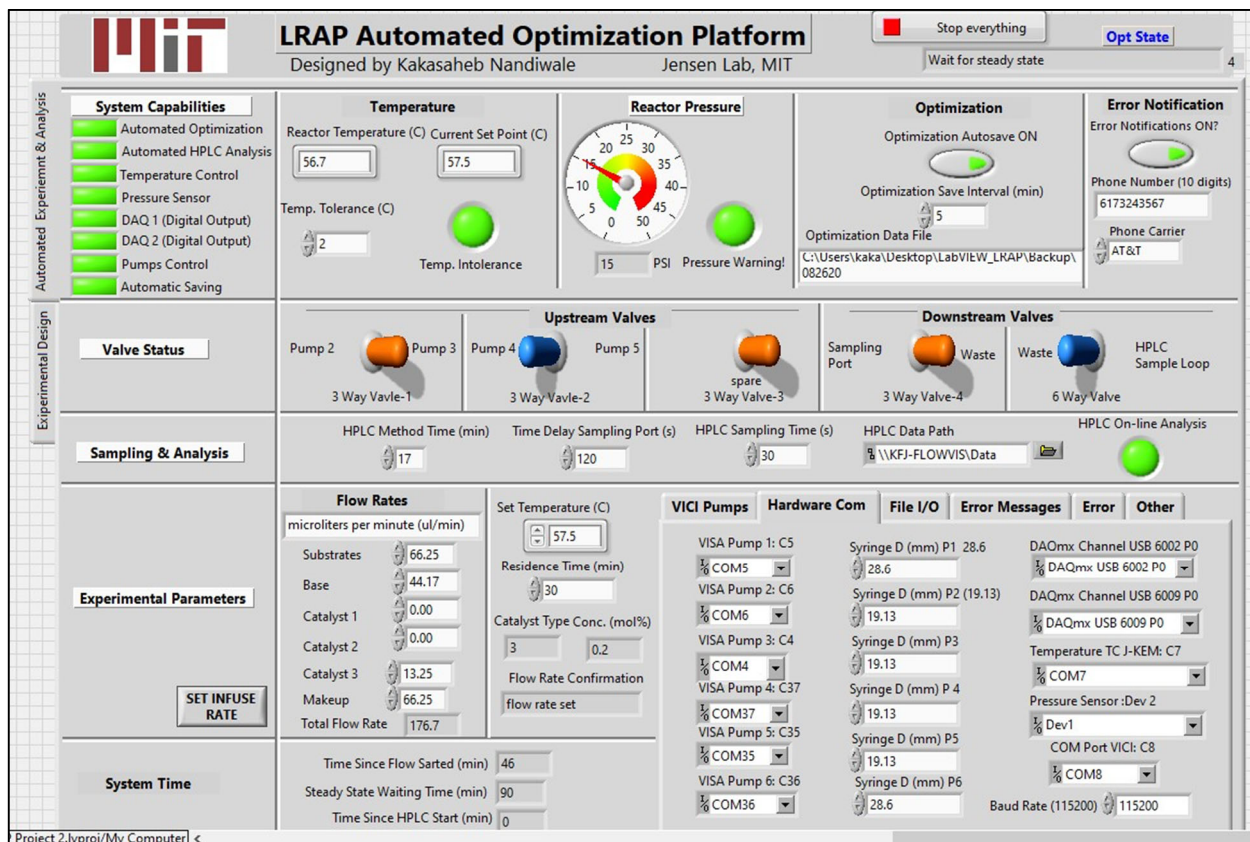
Figure S3. LabVIEW VI user interface for MINLP DoE driven automated optimization.

Prior to the start of optimization campaign, all the regent vials are degassed and connected to the pumps. The CSTR cascade is prefilled with the degassed acetonitrile (MeCN) and pressurized by setting the back pressure regulator (BPR) to the desired pressure with the Alicat Scientific pressure controller connected to the N_2 cylinder. The automated optimization is initialized by activating 'Optimization ON' switch on the LabVIEW VI user interface (Figure S4).

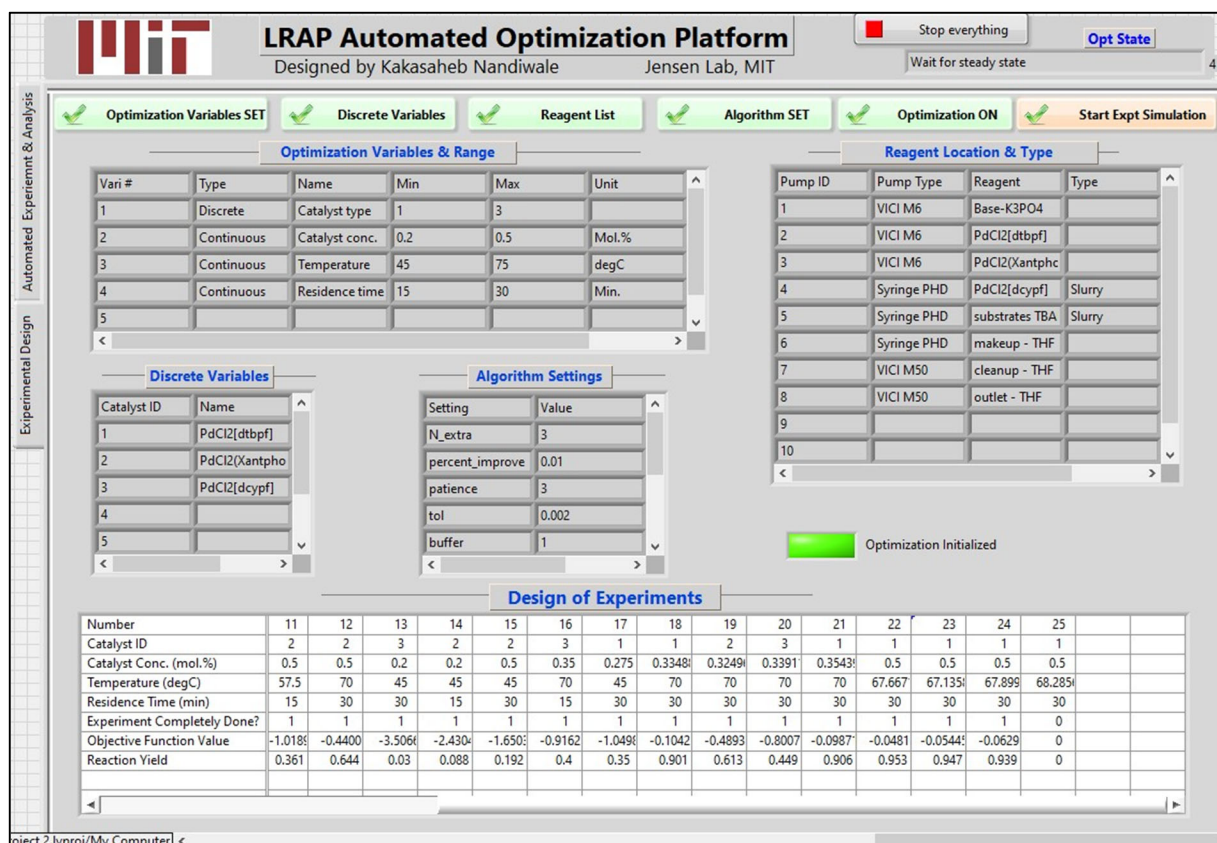| Number	11	12	13	14	15	16	17	18	19	20	21	22	23	24	25
Catalyst ID	2	2	3	2	2	3	1	1	2	3	1	1	1	1	1
Catalyst Conc. (mol.%)	0.5	0.5	0.2	0.2	0.5	0.35	0.275	0.3348	0.3249	0.3391	0.3543	0.5	0.5	0.5	0.5
Temperature (degC)	57.5	70	45	45	45	70	45	70	70	70	70	67.667	67.135	67.899	68.285
Residence Time (min)	15	30	30	15	30	15	30	30	30	30	30	30	30	30	30
Experiment Completely Done?	1	1	1	1	1	1	1	1	1	1	1	1	1	1	0
Objective Function Value	-1.018	-0.4400	-3.506	-2.430	-1.650	-0.9162	-1.049	-0.1042	-0.4893	-0.8007	-0.0987	-0.0481	-0.0544	-0.0629	0
Reaction Yield	0.361	0.644	0.03	0.088	0.192	0.4	0.35	0.901	0.613	0.449	0.906	0.953	0.947	0.939	0

Figure S4. Optimization campaign of Example 1: LabVIEW VI user interface showing optimization variables, reagent location and type, algorithm settings, and MINLP DoE table with results.

Simplified schematic of an automated experimentation is shown in Figure S5. Detailed explanation about the execution and process of an optimization algorithm can be found elsewhere.[3-5] Once the optimization is initialized, the LabVIEW message box provides two options either to perform new optimization with D-optimal DoE or to restore from the previously saved data log file (Figure S5). This triggers MATLAB either to perform mixed-integer nonlinear program (MINLP) algorithm driven DoE or to execute the previously saved DoE data log file. After this selection another message box appears asking user's input to start the automated experimentation. Then the LabVIEW code uses the MATLAB function to select the discrete variable candidate based on the DoE table and to calculate the flow rates based on the reagent

concentration in the stock vials, desired concertation of the reagents in the reactor, reactor volume, and the residence time. The LabVIEW VI parses the desired reaction conditions to perform an automated experiment from the DoE table including flow rates, reaction temperature, residence time, brightness of the LED array etc., to the respective hardware.
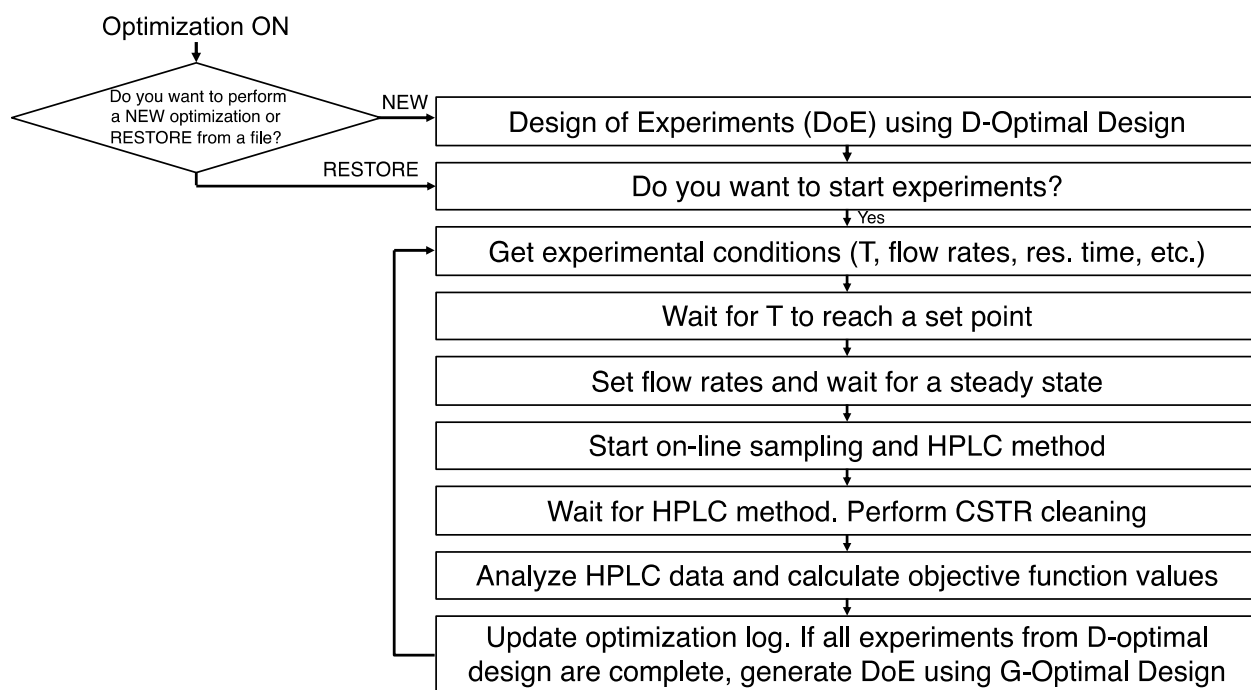

Figure S5. Schematic of LabVIEW VI loops for automated optimization.

The Proportional-integral-derivative (PID) temperature control sets the desired temperature. In case of optimization of photochemical reaction, at this time the irradiation with LED array with the desired brightness from the DoE table is also started. The thermocouple is attached at the back of the CSTR cascade to accurately measure the reactor temperature. Heating and cooling of the CSTR cascade was achieved by the Omega heating cartridges and Peltier cooler (thermo-electric cooling), respectively. Once the set temperature within the tolerance of ~2 °C is reached, the pump flow rates are started indicating the start of the flow experiment. The flow run is continued for ~3 residence times to achieve the steady state.
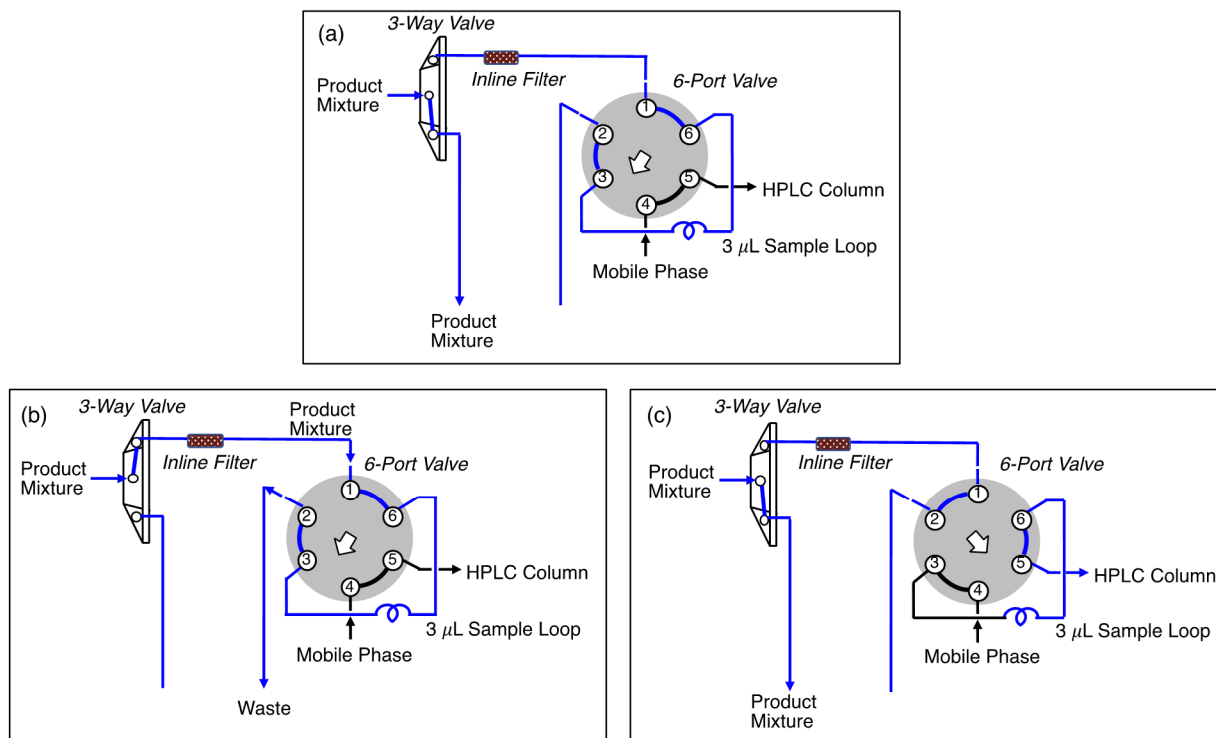
9

Figure S6. Positions of 3-way and 6-port valves during an inline sampling: (a) flow run during the normal operation, (b) sampling to fill the sample loop with the product mixture, and (c) injection of product mixture from the sample loop to the HPLC column.

Automated inline sampling and online HPLC is controlled with the LabVIEW. While waiting for the steady state, the 3-way valve and 6-port valve are positioned as shown in the Figure S6(a). Once the steady state is achieved, the LabVIEW switches the 3-way valve to the position shown in Figure S6(b). This allows flow of the product mixture sample from the CSTR cascade through an inline filter and the external 3 μL sample loop connected to 6-port valve, while the carrier directly to the chromatographic column. This position is maintained for ~2 minutes, to allow the sample loop to fill completely several times and minimize the carryover from the previous sampling. The 6-port valve is then switched to the position shown in Figure S6(c), the sample contained in the sample loop is injected onto the HPLC column, by the mobile phase flowing in an opposite direction (backflush) through the sample loop. At the same time LabVIEW control triggers the HPLC method start. After 30 seconds of online sample injection, the 3-way valve is

switched to the position shown in Figure S6(c). Typical HPLC method was ~16 minutes, once the HPLC method is started the LabVIEW stops flow rates of reagents into the CSTR cascade, heating/cooling, and irradiation with LED array etc., indicating the completion flow run. The time required for the HPLC analysis is utilized to clean the CSTR cascade. During the HPLC method time, the LabVIEW code is set to automatically start the flow of solvent or combination of solvents into the CSTR cascade. This ensures each flow run is performed with the clean slate of reactor.

Once the HPLC analysis method is complete, the Chemstation automatically integrates the resulting chromatogram and saves a report excel sheet under a specified path (HPLC Data Path) (Figure S3). The LabVIEW code checks this directory for the newest Excel file. The MATLAB function is used to read the excel file and to import the product/reactant peak area and calculate the reaction yield/selectivity and objective function. In case, if no product peak was detected in the HPLC report excel file, a value of 0.000001 was assigned to yield/selectivity and objective function value.[3] This helps to avoid undefined values due to the logarithmic scaling of objective function in the case of a 0% reaction yield/selectivity.

After the calculation of objective function values, the LabVIEW code updates the DoE table and optimization date log file, and stops the flow of the pumps used for cleaning the CSTR cascade. The 6-port valve is also reset to the position shown in the Figure S6(a). If the all the experimental from the D-optimal DoE are complete, the G-optimal DoE is performed. The iterative loop is continued to achieve the reaction self-optimization, while performing automated DoE, experimentation, and online sampling and analysis (Figure S5).

Case study 1. Optimization of a Suzuki-Miyaura cross-coupling involving solid substrates and catalyst

The Suzuki-Miyaura cross-coupling step in Meristinib synthesis having solid substrates and catalyst is used an model example to perform automated MINLP optimization (Scheme 1).[6]
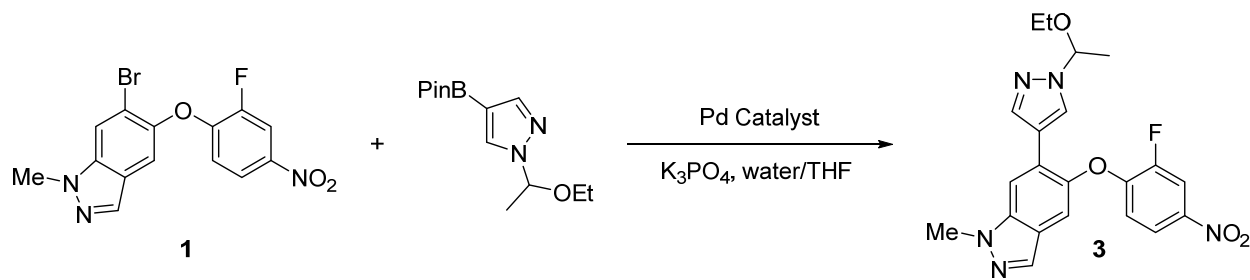
Scheme 1. Suzuki-Miyaura cross-coupling step in Meristinib synthesis.

Preparation of reagent stocks and pump ID:

Pump 1 (VICI M6): K_3PO_4 (9.552 g, 45.0 mmol) in 30 mL H_2O (Stock conc.: 1.5 M)

Pump 2 (VICI M6): $PdCl_2$[dtbpf] (Catalyst 1) (48.88 mg, 0.75 mmol) in 25 mL THF (Stock conc.: 0.0015 M).

Pump 3 (VICI M6): $PdCl_2$(Xantphos) (Catalyst 2) (56.7 mg, 0.075 mmol) in 25 mL THF (Stock conc.: 0.0015 M).

Pump 4 (Syringe - slurry): $PdCl_2$[dcypf] (Catalyst 3) (56.7 mg, 0.075 mmol) in 25 mL THF (Stock conc.: 0.0015 M).

Pump 5 (Syringe - slurry): **1 (**4.394 g, 12.0 mmol), **2** (3.513 g, 13.2 mmol), anisole (200 μL, 1.84 mmol, internal standard for HPLC), TBABr (193.42 mg, 0.6 mmol, internal standard for NMR) in 40 mL THF.

Pump 6 (Syringe): THF – connected at the inlet of CSTR cascade. This is used as a makeup solvent.

Pump 7 (VICI M50): THF – connected at the inlet of CSTR cascade. This is used for reactor prefilling and cleaning the reactor after each run.

Pump 8 (VICI M50): THF – This stream is connected at the outlet of the CSTR cascade with T-connection. This solvent stream is helps to dissolve solids coming out of the CSTR cascade. This stream also helps to dilute the product mixture prior to the online sampling and HPLC analysis.
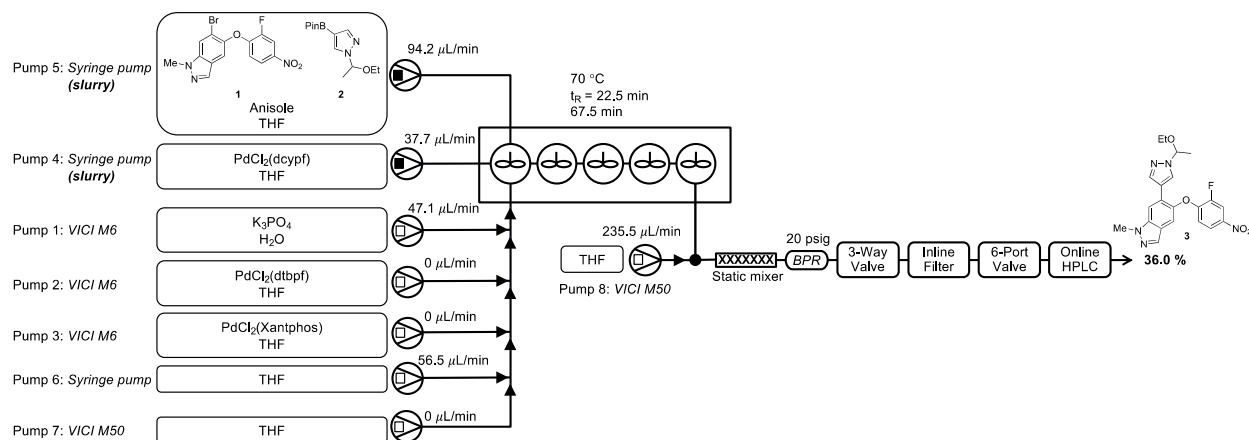

Figure S7. Schematic of system for automated MINLP optimization of Suzuki-Miyaura cross-coupling reaction example involving solid substrates and catalyst.

Under flow conditions: Flow reactions were performed on an automated optimization platform (Figure S1). Stainless-steel syringe with slurry contains a PTFE coated magnetic stir bar, which is stirred by magnetic stirrer to keep slurry uniformly in suspension. All the flow runs in the CSTR cascade were carried out with the constant **1 (**0.15 M, 1.0 equiv.), **2** (1.1 equiv.), anisole (0.15 equiv.), TBABr (0.05 equiv.), K_3PO_4 (2.5 equiv.), and Pd-catalyst (0.005 equiv.) in H_2O:THF (1:4) solvent. Pd-catalyst concentration was varied from 0.2 mol.% to 0.5 mol.%). THF was used as makeup solvent to achieve constant stoichiometry of reagents, catalyst, and solvent. HPLC data was collected on an Agilent 1260 HPLC.

HPLC method: Zorbax Bonus – RP, 4.6 X 150 mm, 3.5 μM particle size. 1.0 mL/min flow, and 25 °C column temperature, detect at 294 nm, solvent A = 1 mL/L TFA in water, and solvent B =

1 mL/L TFA in acetonitrile. Gradient elution (min): T(0) 95%A to 95%B at T(12.0), hold at 95% B until T(14.0) to 95% A at T(14.1), 16 min run time.

Figure S7 shows all the pumps along with contents used for the optimization run. LabVIEW VI used for experimental planning of automated optimization campaign is shown in Figure S4.

Table S3: DoE and experimental results for optimization of Suzuki-Miyaura cross-coupling.

Entry	Discrete Variable (Catalyst) ID	Catalyst Conc. (mol.%)	Temperature (°C)	Residence Time (min)	Yield of 3 (%)
1	3	0.2	70	22.5	36.0
2	1	0.5	45	15	30.2
3	3	0.35	45	15	2.3
4	1	0.2	70	30	88.4
5	3	0.5	57.5	30	14.8
6	2	0.27	57.5	22.5	34.7
7	2	0.2	70	15	40.2
8	1	0.2	57.5	15	41.0
9	1	0.5	70	18.7	81.8
10	3	0.5	45	22.5	4.1
11	2	0.5	57.5	15	36.1
12	2	0.5	70	30	64.4
13	3	0.2	45	30	3.0
14	2	0.2	45	15	8.8
15	2	0.5	45	30	19.2
16	3	0.35	70	15	40.0
17	1	0.27	45	30	35.0
18	1	0.33	70	30	90.1
19	2	0.32	70	30	61.3
20	3	0.34	70	30	44.9
21	1	0.35	70	30	90.6
22	1	0.5	67.7	30	95.3
23	1	0.5	67.1	30	94.7
24	1	0.5	67.9	30	93.9
25	1	0.5	68.3	30	94.2
26	1	0.5	68.2	30	93.0
Optimum Projected	1	0.5	68.2	30	94.1

The DoE based on D-Optimal and G-Optimal along with the experimental results were shown in Table S3. The reaction conditions and flow rates used for the Run 1 (Table S3, entry 1) are shown in Figure S7 as an example of a flow experiment.

Quadratic response surface model parameters for suzuki-miyaura coupling

The quadratic response surface model for the Suzuki-Miyaura coupling example is given by

$$\ln Y = y_1\left(\theta_1 + \theta_2\hat{T}\right) + y_2\left(\theta_3 + \theta_4\hat{T}\right) + y_3\left(\theta_5 + \theta_6\hat{T}\right) + \theta_7\hat{C}_{cat} + \theta_8\hat{t}_{res} +$$

$$\theta_9\hat{C}_{cat}\hat{T} + \theta_{10}\hat{C}_{cat}\hat{t}_{res} + \theta_{11}\hat{t}_{res}\hat{T} + \theta_{12}\hat{C}_{cat}^2 + \theta_{13}\hat{t}_{res}^2 + \theta_{14}\hat{T}^2$$

The terms are defined below.

Table S4. Definitions of terms in quadratic response surface model (Example 1).

| Term	Definition
Y	Yield expressed as a fraction (between 0-1)
y_i	Equal to 1 when catalyst i (1,2, or 3) is present, 0 otherwise.
$\hat{T}$	Transformed and scaled temperature variable (between -1 and 1): $$\hat{T} = 2\left(\frac{T^{-1} - T_{min}^{-1}}{T_{max}^{-1} - T_{min}^{-1}}\right) - 1$$ where T is temperature in Kelvin.
$\hat{C}_{cat}$	Transformed and scaled catalyst concentration variable (between -1 and 1): $$\hat{C}_{cat} = 2\left(\frac{\ln C_{cat} - \ln C_{cat,min}}{\ln C_{cat,max} - \ln C_{cat,min}}\right) - 1$$ where C_{cat} is catalyst conc. in mol%.
$\hat{t}_{res}$	Transformed and scaled residence time variable (between -1 and 1): $$\hat{t}_{res} = 2\left(\frac{\ln t_{res} - \ln t_{res,min}}{\ln t_{res,max} - \ln t_{res,min}}\right) - 1$$ where t_{res} is residence time in minutes.

θ_j are the model parameters fitted to the experimental data using weighted (by yield) least squares regression whose values and uncertainties are given below.

**Table S5.** Values and uncertainties of model parameters (Example 1).

Parameter	Coefficient for term	Value	Standard Error (±)
θ_1	Catalyst 1-specific constant	-0.5636	0.0500
θ_2	Catalyst 1-specific temperature	0.5050	0.0224
θ_3	Catalyst 2-specific constant	-1.1187	0.0445
θ_4	Catalyst 2-specific temperature	0.6734	0.0319
θ_5	Catalyst 3-specific constant	-2.0953	0.0581
θ_6	Catalyst 3-specific temperature	1.3543	0.0480
θ_7	Catalyst conc.	0.1422	0.0183
θ_8	Residence time	0.1659	0.0169
θ_9	Catalyst conc. × Temperature	-0.0365	0.0232
θ_{10}	Catalyst conc. × Residence time	-0.0671	0.0174
θ_{11}	Residence time × Temperature	-0.0458	0.0186
θ_{12}	Catalyst conc. squared	-0.0018	0.0234
θ_{13}	Residence time squared	0.0420	0.0345
θ_{14}	Temperature squared	-0.1999	0.0341

Case study 2. Optimization of a photoredox reaction involving a solid inorganic base

In view to test the solid handling capability of CSTR cascade, the suspension containing 6.8 wt.% Cs_2CO_3 (75 - 90 μm) in acetonitrile is used. Consistent mass outflow of slurry at the outlet of CSTR cascade was observed within an experimental error (Figure S8).
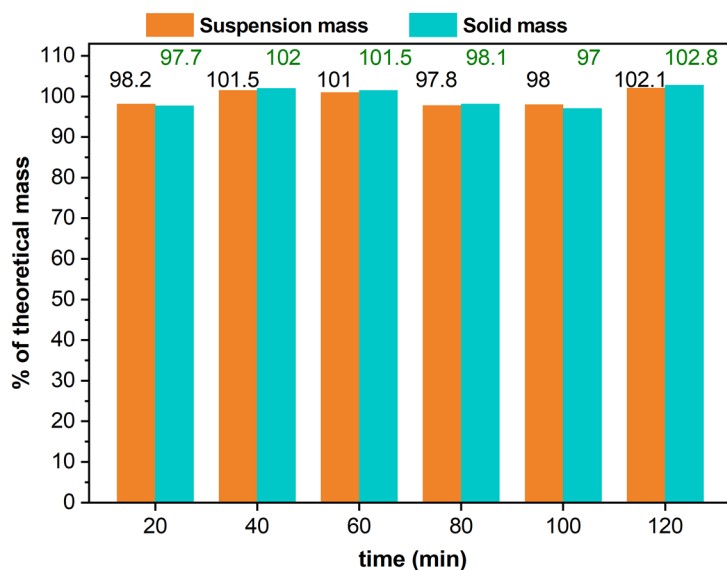
Figure S8: Mass outflow of slurry at the outlet of CSTR cascade.

16

Metallaphotoredox-catalyzed sp^3-sp^3 cross-coupling of carboxylic acids with alkyl halides is shown in Scheme 3.[7]
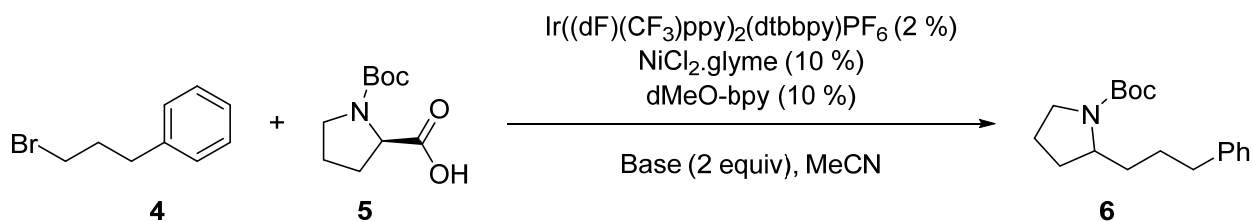
Scheme 3. Photoredox cross-coupling reaction for optimization

Preparation of reagent stocks and arrangement of pumps for the planning of automated optimization campaign is shown in Figure S9.
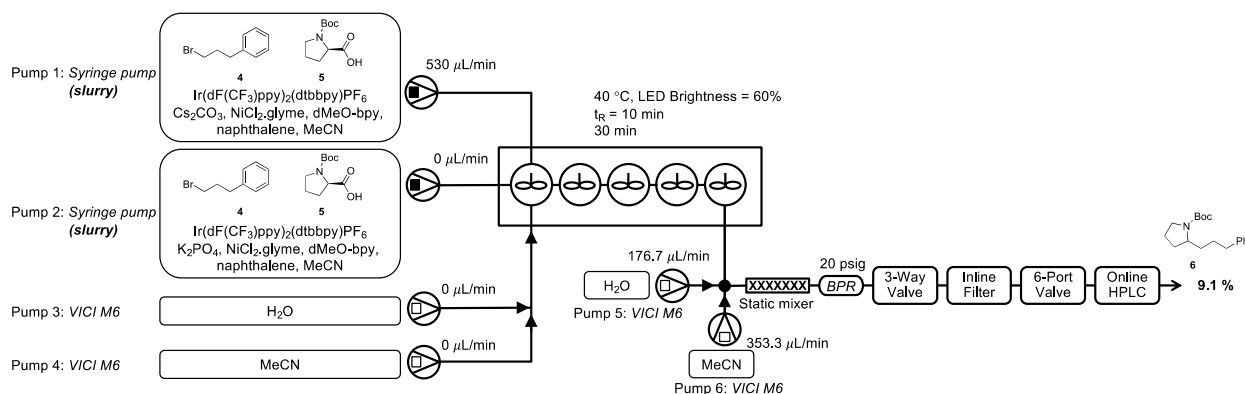

Figure S9. Schematic of system for automated MINLP optimization of Photoredox cross-coupling reaction.

Preparation of reagent stocks and pump ID:

Pump 1 (Syringe - slurry): Cs$_2$CO$_4$ (1.02 g, 3.12 mmol, 2.0 equiv.), (3-bromopropyl)benzene **4** (311 mg, 1.56 mmol, 1.0 equiv.), (tert-butoxycarbonyl)-L-proline **5** (504 mg, 2.34 mmol, 1.5 equiv.), Ir((DF)(CF$_3$)ppy)$_2$(dtbbpy)PF$_6$ (35 mg, 0.03 mmol, 0.02 equiv.), dMeO-bpy (33.7 mg, 0.1 eq. 0.016 mmol, 0.1 equiv.), NiCl$_2$.glyme (34.3 mg, 0.156 mmol, 0.1 equiv.), and naphthalene (20 mg, 0.156 mmol, 0.1 equiv., internal standard for HPLC) in 30 mL MeCN.

Pump 2 (Syringe - slurry): K$_3$PO$_4$ (431 mg, 3.12 mmol), (3-bromopropyl)benzene **4** (311 mg, 1.56 mmol, 1 equiv.), (tert-butoxycarbonyl)-L-proline **5** (504 mg, 2.34 mmol, 1.5 equiv.), Ir((DF)(CF$_3$)ppy)$_2$(dtbbpy)PF$_6$ (35 mg, 0.03 mmol, 0.02 equiv.), dMeO-bpy (33.7 mg, 0.1 eq. 0.016 mmol, 0.1 equiv.), NiCl$_2$.glyme (34.3 mg, 0.156 mmol, 0.1 equiv.), and naphthalene (20 mg, 0.156 mmol, 0.1 equiv., internal standard for HPLC) in 30 mL MeCN.

Pump 3 (VICI M6): H$_2$O – connected at the inlet of the CSTR cascade. This is used for the cleaning of CSTR cascade after each run. This stream helps to rapidly dissolve the base in the CSTR cascade after each run and clean the reactor.

Pump 4 (VICI M6): MeCN – connected at the inlet of CSTR cascade. This stream is used for reactor prefilling the CSTR cascade before start of reaction. In addition, this stream is also used for cleaning of the reactor after each run.

Both **Pump 3** and **Pump 4** are used for cleaning the CSTR cascade after each run with H$_2$O:MeCN (1:2, achieved by adjusting the flow rates). This solvent stream (H$_2$O:MeCN = 1:2) was found to be efficient in dissolving base (Cs$_2$CO$_4$ or K$_3$PO$_4$) and at the same time maintaining the other organic reagents in the homogeneous phase.

Pump 5 (VICI M6): H$_2$O – This stream is connected at the outlet of the CSTR cascade through cross connector. This helps to dissolve solids coming out of the reactor.

Pump 6 (VICI M6): MeCN – This stream is connected at the outlet of the CSTR cascade through cross connector. This helps to dissolve solids coming out of the reactor. In addition, this stream also helps to dilute the product mixture prior to the online sampling and inline HPLC analysis.

HPLC (Agilent 1260) method: Zorbax Bonus – RP, 4.6 X 150 mm, 3.5 µM particle size. 1.0 mL/min flow, and 25 °C column temperature, detect at 280 nm, solvent A = 1 mL/L TFA in acetonitrile, and solvent B = 1 mL/L TFA in water. Gradient elution (min): T(0) 50%A to 90%B at T(10.0), T (10.0) 10%A to 50%B at T(16.0), and 17 min run time.

Flow reactions were performed on newly developed automated optimization platform (Figure 2). Figure S9 shows all the pumps along with contents used for the optimization run. LabVIEW VI user interface showing optimization variables, reagent location and type, algorithm settings, and MINLP DoE table with results is shown in Figure S10. The DoE based on D-Optimal and G-Optimal along with the experimental results were shown in Table S6. The reaction conditions and flow rates used for the Run 1 (Table S6, entry 1) are shown in Figure S9 as an example of a flow experiment.
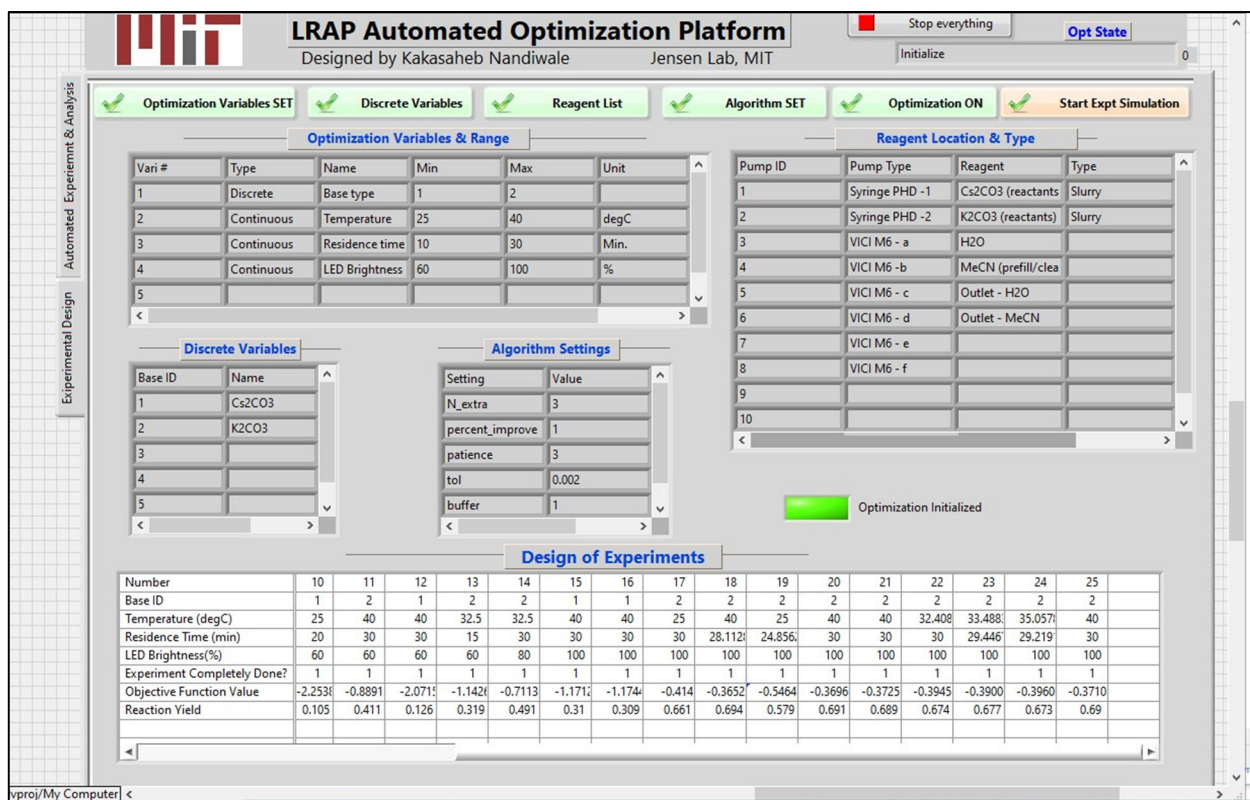

Figure S10. LabVIEW VI user interface for MINLP optimization campaign of photochemical reaction.

Table S6. MINLP DoE and experimental results for optimization of photochemical reaction.

Entry	Discrete Variable (Base) ID	Temperature (°C)	Residence Time (min)	LED Brightness (%)	Yield of 6 (%)
1	1	40	10	60	**9.1**
2	1	32.5	10	100	**11.5**
3	2	25	10	60	**20.0**
4	2	25	30	60	**38.4**
5	2	40	10	100	**25.9**
6	1	25	30	100	**27.7**
7	2	25	15	100	**56.8**
8	1	40	15	80	**17.8**
9	1	25	10	80	**11.2**
10	1	25	20	60	**10.5**
11	2	40	30	60	**41.1**
12	1	40	30	60	**12.6**
13	2	32.5	15	60	**31.9**
14	2	32.5	30	80	**49.1**
15	1	40	30	100	**31.0**
16	1	40	30	100	**30.9**
17	2	25	30	100	**66.1**
18	2	40	28	100	**69.4**
19	2	25	25	100	**57.9**
20	2	40	30	100	**69.1**
21	2	40	30	100	**68.9**
22	2	32	30	100	**67.4**
23	2	33	29	100	**67.7**
24	2	35	29	100	**67.3**
25	2	40	30	100	**69.0**
Optimum Projected	2	38.7	29.9	100	**68.9**

Quadratic response surface model parameters for photochemical reaction

The quadratic response surface model for the photoredox coupling example is given by

$$\ln Y = y_1\left(\theta_1 + \theta_2\hat{T}\right) + y_2\left(\theta_3 + \theta_4\hat{T}\right) + \theta_5\hat{t}_{res} + \theta_6\hat{L} +$$

$$\theta_7\hat{t}_{res}\hat{T} + \theta_8\hat{t}_{res}\hat{L} + \theta_9\hat{L}\hat{T} + \theta_{10}\hat{t}_{res}^2 + \theta_{11}\hat{T}^2 + \theta_{12}\hat{L}^2$$

The terms are defined below.

**Table S7.** Definitions of terms in quadratic response surface model (Example 2).

Term	Definition
Y	Yield expressed as a fraction (between 0-1)
y_i	Equal to 1 when base i (1 or 2) is present, 0 otherwise.
$\hat{T}$	Transformed and scaled temperature variable (between -1 and 1): $$\hat{T} = 2\left(\frac{T^{-1} - T_{min}^{-1}}{T_{max}^{-1} - T_{min}^{-1}}\right) - 1$$ where T is temperature in Kelvin.
$\hat{t}_{res}$	Transformed and scaled residence time variable (between -1 and 1): $$\hat{t}_{res} = 2\left(\frac{\ln t_{res} - \ln t_{res,min}}{\ln t_{res,max} - \ln t_{res,min}}\right) - 1$$ where t_{res} is residence time in minutes.
$\hat{L}$	Transformed and scaled LED brightness variable (between -1 and 1): $$\hat{L} = 2\left(\frac{\ln L - \ln L_{min}}{\ln L_{max} - \ln L_{min}}\right) - 1$$ where L is LED brightness in %.

θ_j are the model parameters fitted to the experimental data using weighted (by yield) least squares regression whose values and uncertainties are given below.

Table S8. Values and uncertainties of model parameters (Example 2).

Parameter	Coefficient for term	Value	Standard Error ($\pm$)
θ_1	Base 1-specific constant	-1.7468	0.1006
θ_2	Base 1-specific temperature	0.0396	0.0556
θ_3	Base 2-specific constant	-0.8502	0.0904
θ_4	Base 2-specific temperature	-0.0172	0.0397
θ_5	Residence time	0.3506	0.0383
θ_6	Brightness	0.2524	0.0327
θ_7	Residence time × Temperature	0.0594	0.0376
θ_8	Residence time × Brightness	0.0482	0.0383
θ_9	Brightness × Temperature	-0.0153	0.0308
θ_{10}	Residence time squared	-0.2136	0.0758
θ_{11}	Temperature squared	0.0115	0.0468
θ_{12}	Brightness squared	0.0083	0.0775

Example 3. Automated Bayesian optimization of multiphase diastereoselective metallaphotoredox cross coupling
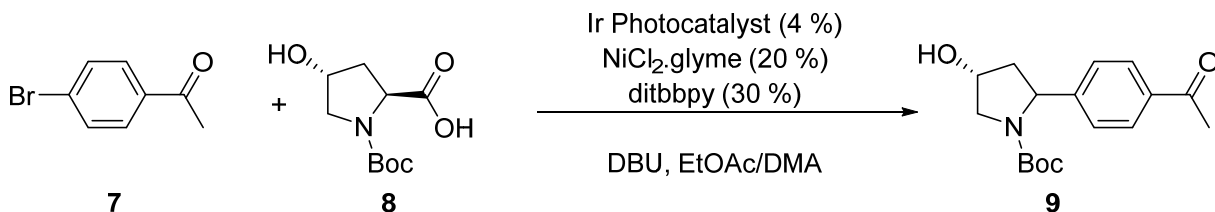
Scheme 3. Diastereoselective metallaphotoredox cross coupling

Preparation of reagent stocks and pump ID:

Pump 1 (Syringe - slurry): **7** (1.33 g, 6.70 mmol), NiCl$_2$.glyme (147.21 mg, 0.67 mmol), 4,4′-di-*tert*-butyl-2,2′-dipyridyl (269.75 g, 1 mmol), naphthalene (86 mg, 0.67 mmol, internal standard for HPLC), and DBU (3.06 g, 20.1 mmol), and 10 mL DMA.

Pump 2 (VICI M6): **8** (4.65 g, 20.1 mmol), Photocatalyst (1) (152 mg, 0.134 mmol), 5 mL DMA.

Pump 3 (VICI M6): **8** (4.65 g, 20.1 mmol), Photocatalyst (2) (122 mg, 0.134 mmol), 5 mL DMA.

Pump 4 (VICI M6): Ethyl acetate

Pump 5 (VICI M6): DMA**:** reactor prefilling, reaction solvent, and cleaning the CSTR cascade after each run.

Pump 6 (VICI M6): Aq. MeCN (H$_2$O:MeCN = 1:1) - This stream is connected at the outlet of the CSTR cascade through T-connector. This helps to dissolve solids coming out of the reactor. In addition, this stream also helps to dilute the product mixture prior to the inline sampling and online HPLC analysis.
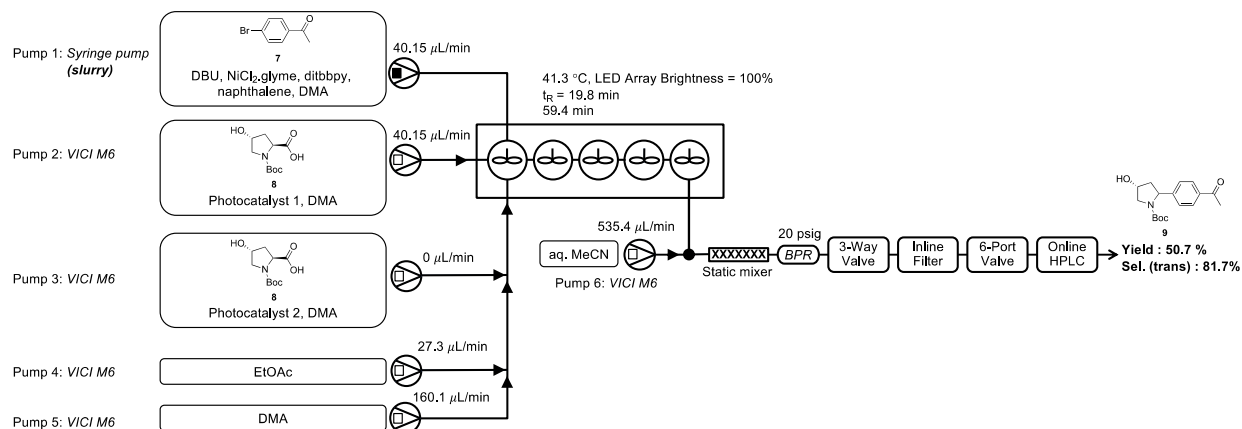
Figure S11. Schematic of system for Bayesian optimization of diastereoselective metallaphotoredox cross coupling.

Figure S11. Shows setup for Bayesian optimization design for diastereoselective metallaphotoredox cross coupling. LabVIEW VI was updated to perform automated DoE based on Bayesian optimization algorithm, automated experimentation, online sampling, and automated analysis with HPLC.

HPLC (Agilent 1260) method: Zorbax Bonus – RP, 4.6 X 150 mm, 3.5 μM particle size. 1.0 mL/min flow, and 25 °C column temperature, detect at 254 nm, solvent A = 1 mL/L TFA in acetonitrile, and solvent B = 1 mL/L TFA in water. Gradient elution (min): T(0) 20%A to 60%B at T(1.0), T (1.0) 40%A to 50%B at T(10.0), T(10.0) 50%A to 5%B at T(12.0), T(12.0) 95%A to 95%B(T14.0), T (14.0) 5%A to 50%B at T (15.0), 16 min run time.

Under flow conditions: Flow reactions were performed on an automated optimization platform shown in Figure 2. All the flow runs in the CSTR cascade were carried out with the constant concentration of **7** of 0.1 M, with relative proportions of the ethyl acetate: DMA mixture adjusted by varying the relative flow rates of pumps 4 and 5. The first eight experiments were initialization runs, followed by new runs of batch size = 2 (when duplicate conditions were suggested, the second

23

was eliminated). The flow rates shown in Figure are for run 1 from Bayesian optimization DoE Table 1.

Dragonfly Bayesian optimization algorithm

The Dragonfly open-source Bayesian optimization package developed by Kandasamy et al,[8, 9] constructs a Gaussian process surrogate model to describe the relationship between input variables and objective functions. Both continuous and discrete variables can be defined in the optimization domain. In the initialization phase, a space-filling design of experiments is generated using Latin hypercube sampling (LHS) for continuous variables and random sampling for discrete variables.
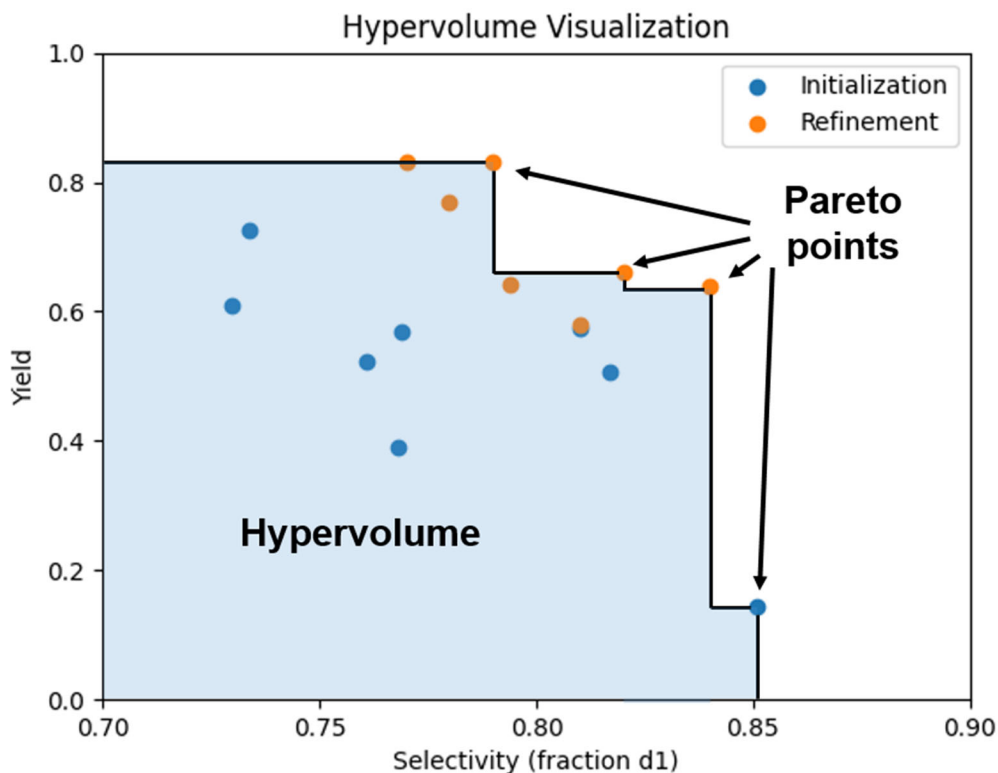

Figure S12. Visualization of hypervolume enclosed by Pareto optimal points for case study 3 involving Bayesian two-objective optimization of a multiphase diastereoselective metallaphotoredox cross-coupling.

The initialization was repeated until four initialization reactions with each photocatalyst 1 and 2 were included in the initial set for equal coverage. Once the initialization results are returned to

the algorithm, either the upper confidence bound (UCB) or Thompson sampling (TS) acquisition functions are selected (with equal probability) to generate each refinement experiment. A Jupyter notebook demonstrating how to use the Dragonfly Bayesian optimization package is available at: https://github.com/anirudh-nambiar/make-it-system/tree/main/dragonfly_bayesopt_demo.

In multi-objective optimization, the goal is to identify Pareto optimal points that represent the trade-off between potentially conflicting objectives. To find multiple Pareto optimal points, Dragonfly employs a random scalarization strategy,[9] where different weights (relative importance) for each objective are sampled at each refinement iteration and the weighted sum is maximized. To assess algorithm convergence, the hypervolume indicator was utilized. For two objectives, the hypervolume corresponds to the area enclosed by the current Pareto points. The hypervolume was computed using the pymoo Python package (https://pymoo.org/misc/indicators.html), and is visualized in Figure S12.

Product isolation and characterization

In view to isolate the product standards, the system was run at steady-state conditions at the optimal conditions (those from run 13) for 35 minutes. The product during this time period was collected and extracted with ethyl acetate (3 x 30 mL). The layers were separated with a 125 mL separatory funnel, and the organic layer dried over magnesium sulfate. The concentrate was chromatographed using ethyl acetate:heptane to afford the desired product (252 mg, 76 %).

The identity of both *trans* and *cis* stereoisomers of compound **9** were confirmed by comparison with the reported literature spectrum.[10]

9-*trans*:

^{1}H NMR (CDCl$_3$, 400 MHz): δ = 7.91 (d, J = 8.3 Hz, 2H), 7.37 (d, J = 8.1 Hz, 2H), 4.80–5.18 (m, 1H), 4.42–4.59 (m, 1H), 3.88 (br s, 1H), 3.60 (dd, J = 11.8, 3.2 Hz, 1H), 2.59 (s, 3H), 1.98 (dt, J = 13.3, 4.1 Hz, 1H), 1.47 (br s, 3H), 1.19 ppm (br s, 6H).

9-*cis*:

^{1}H NMR (CDCl$_3$, 400 MHz): δ = 7.91 (d, J = 8.3 Hz, 2H), 7.29 (d, J = 8.1 Hz, 3H), 4.86–5.25 (m, 1H), 4.51 (br s, 1H), 3.66–4.09 (m, 2H), 2.60 (s, 3H), 2.42 (br dd, J = 12.7, 6.7 Hz, 1H), 1.93 (ddd, J = 13.4, 8.8, 4.4 Hz, 1H), 1.84 (br s, 1H), 1.44 (br s, 2H), 1.14 ppm (br s, 6H).

References

1. A. Pomberger, Y. Mo, K. Y. Nandiwale, V. L. Schultz, R. Duvadie, R. I. Robinson, E. I. Altinoglu and K. F. Jensen, *Org. Process Res. Dev.*, 2019, DOI: 10.1021/acs.oprd.9b00378.

2. A. Wood, K. Y. Nandiwale, Y. Mo, J. Bo, A. Pomberger, V. Shultz, F. Gallou, K. F. Jensen and B. H. Lipshutz, *Green Chem*, 2020, DOI: 10.1039/D0GC00378F.

3. L. M. Baumgartner, C. W. Coley, B. J. Reizman, K. W. Gao and K. F. Jensen, *React Chem Eng*, 2018, **3**, 301-311.

4. H.-W. Hsieh, C. W. Coley, L. M. Baumgartner, K. F. Jensen and R. I. Robinson, *Org. Process Res. Dev.*, 2018, **22**, 542-550.

5. L. M. Baumgartner, J. M. Dennis, N. A. White, S. L. Buchwald and K. F. Jensen, *Org. Process Res. Dev.*, 2019, **23**, 1594-1601.

6. K. P. Cole, B. M. Campbell, M. B. Forst, J. McClary Groh, M. Hess, M. D. Johnson, R. D. Miller, D. Mitchell, C. S. Polster, B. J. Reizman and M. Rosemeyer, *Org. Process Res. Dev.*, 2016, **20**, 820-830.

7. C. P. Johnston, R. T. Smith, S. Allmendinger and D. W. C. MacMillan, *Nature*, 2016, **536**, 322-325.

8. K. Kandasamy, K. Raju Vysyaraju, W. Neiswanger, B. Paria, C. R. Collins, J. Schneider, B. Poczos and E. P. Xing, *Journal of Machine Learning Research*, 2019, **21**, 1-27.

9. B. Paria, K. Kandasamy and B. Póczos, 2018, arXiv:1805.12168.

10. I. Abdiaj and J. Alcázar, *Bioorganic & Medicinal Chemistry*, 2017, **25**, 6190-6196.